CROSSDRO

Deliverable

4.3. Drought impacts on crops and forests

Lars Eklundh, Hongxiao Jin, Zhanzhang Cai

Department of Physical Geography and Ecosystem Science

Lund University

Contents

1 Introduction

1.1 Background

Drought is a recurring natural hazard that results from a sustained reduction in precipitation. Drought has significant impacts on agricultural production and forest ecosystems worldwide (Ciais *et al.* 2005; Santini *et al.* 2022). In recent decades, drought events have become more frequent and severe in Europe due to climate warming (Cammalleri *et al.* 2020; Naumann *et al.* 2021). From 1981 to 2010, the average annual loss due to drought in Europe was approximately €9 billion, with half of these losses being agricultural (Cammalleri *et al.* 2020; Naumann *et al.* 2021). The most recent European drought, which occurred in 2018-19, had a significant impact on crop yields and forest growth in northern and central Europe (Boergens *et al.* 2020; Conradt *et al.* 2023).

Drought affects multiple aspects of the agricultural sector. Firstly, it reduces crop productivity, which can lead to risks of food insecurity and water scarcity for both livestock and humans (Carrão *et al.* 2016). Furthermore, drought can increase cropland net carbon release into the atmosphere (Humphrey *et al.* 2018), which introduces uncertainties in cropland carbon accounting (Oldfield *et al.* 2022). Additionally, drought stress can make plants more susceptible to pests and diseases, which further reduces crop yields (Maxmen 2013). Drought also has a significant impact on forest ecosystems in Europe. For example, drought stress increased the vulnerability of trees to insect infestations, forest fires, and other disturbances, resulting in forest degradation and loss (Anderegg *et al.* 2015). Furthermore, drought can alter the composition and structure of forest communities, with some species being more resilient to drought than others (Lafleur and Humphreys 2018).

This deliverable is partly compiled from a white paper, *High Resolution Vegetation Phenology and Productivity Use Case: Local Scale Impacts of the2018 Drought on Vegetation in N. Europe*., drafted by the authors for the Copernicus HRVPP project (CLMS 2022).

1.2 Study of 2018 drought using Sentinel-2

1.2.1 The 2018 northern Europe drought

While historically drought has not been widespread in northern Europe, the year 2018 saw a drought that had severe and widespread impacts in northern Europe (Conradt *et al.* 2023). This drought was caused by an exceptionally warm spring and a very dry summer (Peters *et al.* 2020). The drought caused severe losses in crop production in northern and eastern Europe (Beillouin *et al.* 2020). For example, the drought led to the lowest crop yields in Sweden since 1959, including 43% lower yield for grain and 35% lower for oilseeds compared to the last 5 years, and less than half the production of ley to normal (SCB 2018). Additionally, the drought led to forest fires and increased insect attacks on trees. Many forest stands reduced their carbon uptake in 2018 as a consequence of increased heterotrophic respiration (Lindroth *et al.* 2020), and several northern wetlands (mires) turned from carbon sinks to carbon sources (Rinne *et al.* 2020). To visualize the extent and severity of the 2018 drought across Europe, an interactive map of vegetation and drought indices can be found at https://expertonrs.users.earthengine.app/view/eudrought2018 using Google Earth Engine platform.

1.2.2 Sentinel-2 HR-VPP products

In this study, we examine the local-scale impact of the 2018 drought on crops and forests using data from the Pan-Europe Sentinel-2 product High-Resolution Vegetation Phenology and Productivity products (HR-VPP) during period 2017-2020. These products were developed by the Copernicus Land Monitoring Service (CLMS), which provides geographical information on land cover and its changes, land use, vegetation state, water cycle and earth surface energy variables to a wide range of users in Europe and across the world for environmental terrestrial applications. The CLMS is a joint initiative between the European Environment Agency and the European Commission DG Joint Research Centre (JRC).

The HR-VPP products are generated from high-resolution (10m x 10m) Sentinel-2A and Sentinel-2B satellite data, with an average joint revisit time of 5 days. These products cover the entire EEA39 region, which includes 32 member countries, the UK, and 6 cooperating countries in the Western Balkans from January 1, 2017, onwards. The Seasonal Trajectories (ST) product of HRVPP is derived by fitting a function (Cai *et al.* 2017) to the yearly time-series of raw Plant Phenology Index (PPI, Jin and Eklundh 2014) for each pixel per 10-day interval. The Vegetation Phenological and Productivity parameters (VPP) are generated on a yearly basis and provide thirteen metrics up to two growing seasons, such as start of season, end of season, seasonal productivity, etc.

1.3 The aim of the study

The aim of the study is to investigate the instantaneous local impacts of the 2018 drought on crops and forests, while also highlighting the capability of the novel high-resolution HR-VPP products for studying local-scale vegetation dynamics under drought stress. To do so, we used the Standardized Precipitation Evapotranspiration Index (SPEI) developed by Vicente-Serrano et al. (2010), which considers the multitemporal nature of atmospheric water balance (precipitation-minus-potential-evapotranspiration). The SPEI has been widely used in recent analyses of drought impacts on vegetation (e.g. Christopoulou *et al.* 2021; Huang and Wang 2021; Lawal *et al.* 2021; Mokhtar *et al.* ; Zhong *et al.* 2021). We focused on selected areas in six European countries (Belgium, Germany, Denmark, S Sweden, E Sweden, and Finland) to exemplify the local effects of the 2018 drought.

2 Data and methodology

2.1 Data

2.1.1 Drought data

High-temporal and spatial resolution (9 km) climate data from ECMWF ERA5-land reanalysis dataset and the Multi-Source Weighted-Ensemble Precipitation (MSWEP) for calculation of SPEI 3-month and 12-month drought indices at weekly time step.

2.1.2 Crop yield and growth phenology data

Crop field delineations for 2017-2020 for southern Sweden from the Swedish Board of Agriculture. Crop yield statistics from the Swedish Central Bureau of Statistics. HR-VPP phenology parameters and seasonal trajectories from Sentinel-2 at 10 m spatial resolution, 2017-2020 of six tiles (31UFS, 32UPE, 32UPG, 33UUB, 33VWC, 35VLJ) located in central and northern Europe (Figure 1).

2.1.3 Forest data

Forest cover from CLC land cover, updated 2018. Medium resolution growing season parameters (phenology and productivity) from MODIS NBAR data aggregated to 5 km spatial resolution.

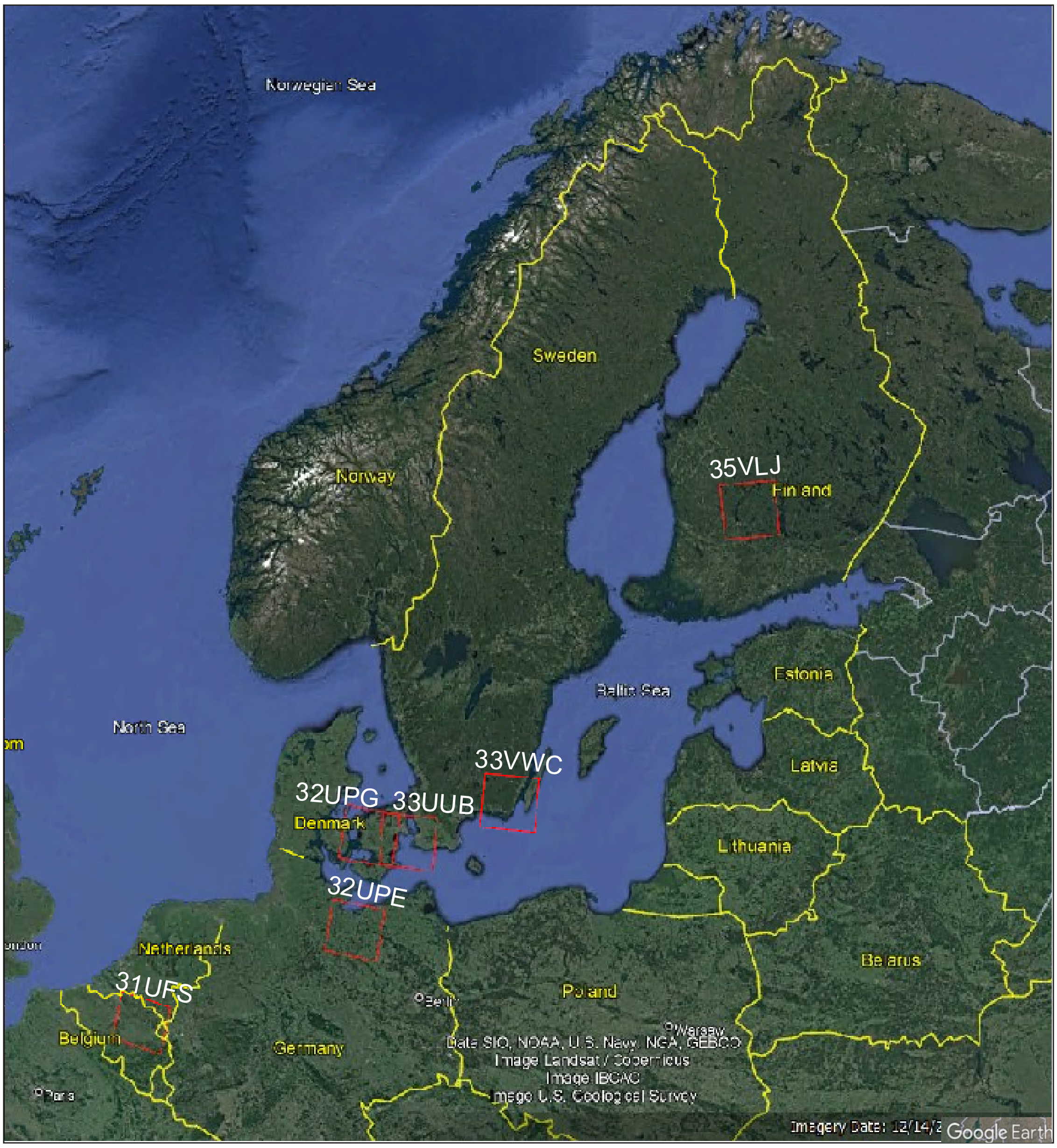

Figure 1. Six selected Sentinel-2 tiles, located in Belgium, Northern Germany, Denmark, southern Sweden, Eastern Sweden, and Central Finland, for the analysis of drought impacts on crops and forests at the local scale.

2.2 Estimation of meteorological drought severity

The SPEI data were used to estimate drought severity in the different test areas. Drought severity is defined as the run sum of SPEI (Dracup *et al.* 1980; Mishra and Singh 2010) over the yearly-averaged growing season in this study. The SPEI was computed using three-parameter log-logistic distribution for the water balance (the difference between precipitation and potential evapotranspiration) following Vicente-Serrano *et al.* (2010). The potential Evapotranspiration (ETo, reference evapotranspiration) was calculated from ERA5-land climate variables using the Penman-Monteith equation following FAO56 (Allen *et al.* 1998).

$$S = \sum_{t=SOS}^{EOS} SPEI_t, \quad (1)$$

$$\hat{S} = S - S_{fit}, \quad (2)$$

where S is the drought severity (i.e. growing season SPEI sum). Sfit and $\hat{S}$ are robust linear trend values and robustly-detrended drought severity values, respectively. The trend was estimated using robust fitting by iteratively reweighted least-squares (Holland and Welsch 1977) to account for trend bias caused by extreme drought events.

Standardized anomalies (z-scores) of drought severity were computed pixel-wise as follows:

$$Z_x = \frac{x-\mu_x}{\sigma_x}, \quad (3)$$

where Zx is the z-score of variable x, µx is the mean of x, and σx is the standard deviation of x. Note that x is the value of robustly detrended drought severity $\hat{S}$, so as to address the issue of varied mean of a non-stationary time series used in the z-score calculation. The standard anomaly of drought severity was computed from SPEI at 3 and 12 months' time scale respectively to address the short-term and long-term climatic drought respectively.

2.3 Analysis of drought effects on local agriculture

We conducted an analysis of the effects of drought on local agriculture in Sentinel-2 tile 33UUB, located in southern Sweden (Figure 2). This area was chosen due to its documented effects of the 2018 drought and availability of relevant data.

Our analysis focused on six common crop types, namely spring barley, rye, autumn wheat, autumn rapeseed, sugar beet, and hayfield, which together account for approximately 75% of the arable land in the region (Figure 3).

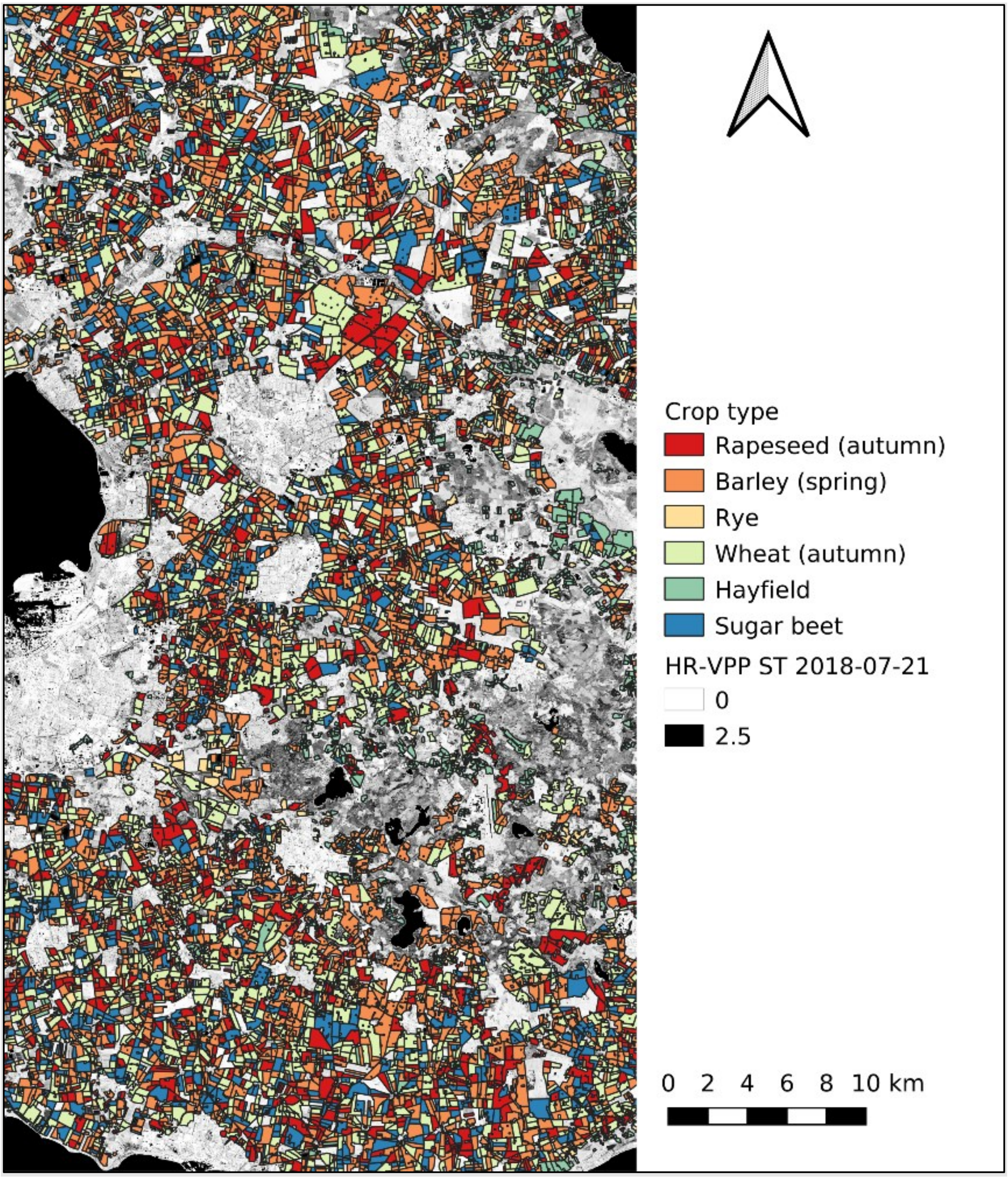

Figure 1. Map of the test area for drought effect on crops, southern Sweden. Source of data: Swedish Board of Agriculture. Reproduced from CLMS (2022) with permission.

To assess the impact of drought on these crops, we examined the following phenological parameters:

- TPROD: the seasonal large integral of PPI, indicative of total seasonal vegetation productivity
- AMPL: seasonal amplitude, indicative of maximum-minimum of vegetation productivity during the season

- LENGTH: season length
- SOSD, EOSD: start and end of season dates: indicative of shifts in the growing season.

We calculated normalized phenological parameters for each crop type between 2017 and 2020.

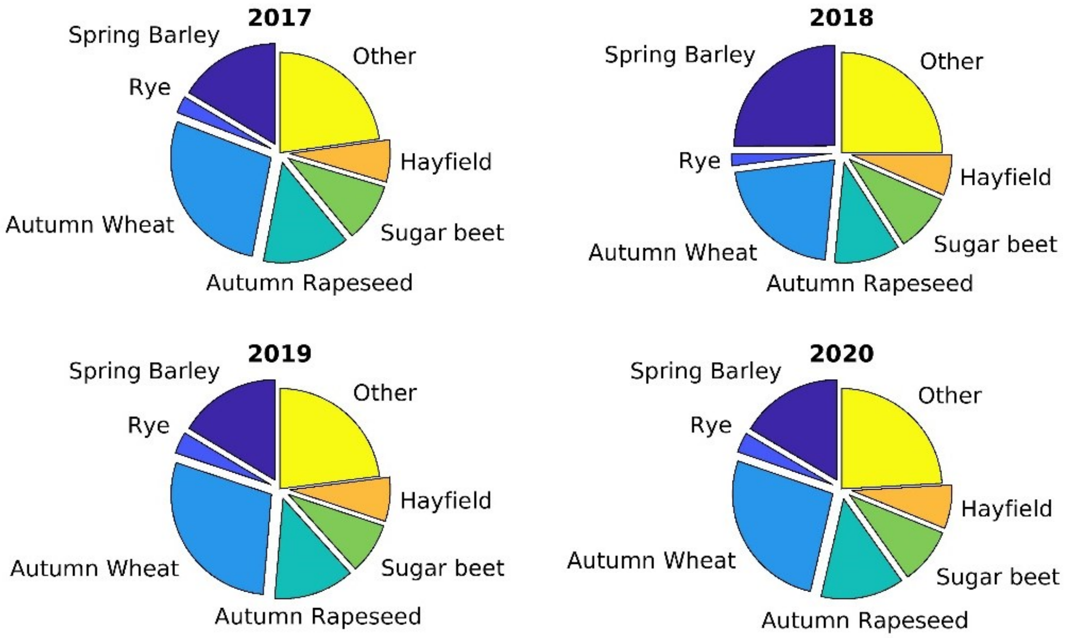

Figure 2. Area cover of most common crops in southern Sweden 2017-2017. Data source: Swedish Board of Agriculture. Reproduced from CLMS (2022) with permission.

Since severe drought can cause the value of PPI to drop to a low level during the growing season, we treated it as one growing season if two separate seasons occurred within a year. As a result, our VPP parameters for a given year were derived from the aggregation of the two seasons, with the SOSD representing the start of the first season, EOSD representing the end of the second season, and LENGTH representing the number of days between SOSD and EOSD.

2.4 Analysis of HR-VPP in forest lands

To analyze the seasonal vegetation productivity of broad-leaved and coniferous forests, we overlaid phenological data at a resolution of 10 m with land cover data from CLC at a resolution of 100 m. We calculated the normalized statistics for the same phenological parameters (TPROD, AMPL, LENGTH, SOSD, EOSD) for each forest type, using the same approach as in section 2.2 for local agriculture.

3 Results

3.1 Drought severity during 2017-2020

In the study areas, 2018 was an exceptionally dry year when compared to the previous 20 years, as evident from the standardized anomaly of drought severity (Z-scores of growing season aggregated SPEI-3), depicted in Figure 4. However, the preceding year, 2017, had positive SPEI values indicating a wetter growing season using short-term accumulation, while 2019 was neutral.

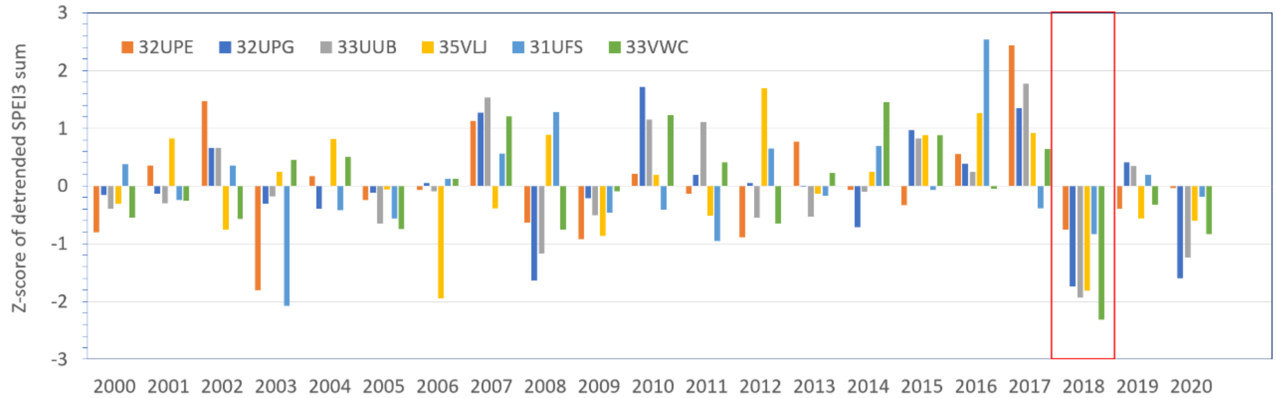

Figure 3. Drought severity (standard anomaly of SPEI3 sum) for each of the study areas 31UFS: Belgium, 32UPE: Germany, 32UPG: Denmark, 33UUB: southern Sweden, 33VWC: SE Sweden, and 35VLJ: Finland. Reproduced from CLMS (2022) with permission.

The drought index SPEI for the study areas is further illustrated in Figure 5 and Figure 6 for SPEI-3 and SPEI-12, respectively. For 2018, the standard anomaly of drought severity calculated from short-term drought index SPEI-3 was very low for the majority of the study areas, especially in Jutland Denmark, Sweden, Norway, and Finland. However, the following years did not indicate general drought, except for Lithuania and a small part of Poland, which had negative SPEI values during 2019. In contrast, drought severity from longer-term drought index SPEI-12 shows a different pattern with low values during 2019, particularly in S. Denmark, N. Germany, Netherlands, Belgium, and the Baltic countries, indicating the sustained effect of the 2018 drought and its impact on water availability at deeper soil levels.

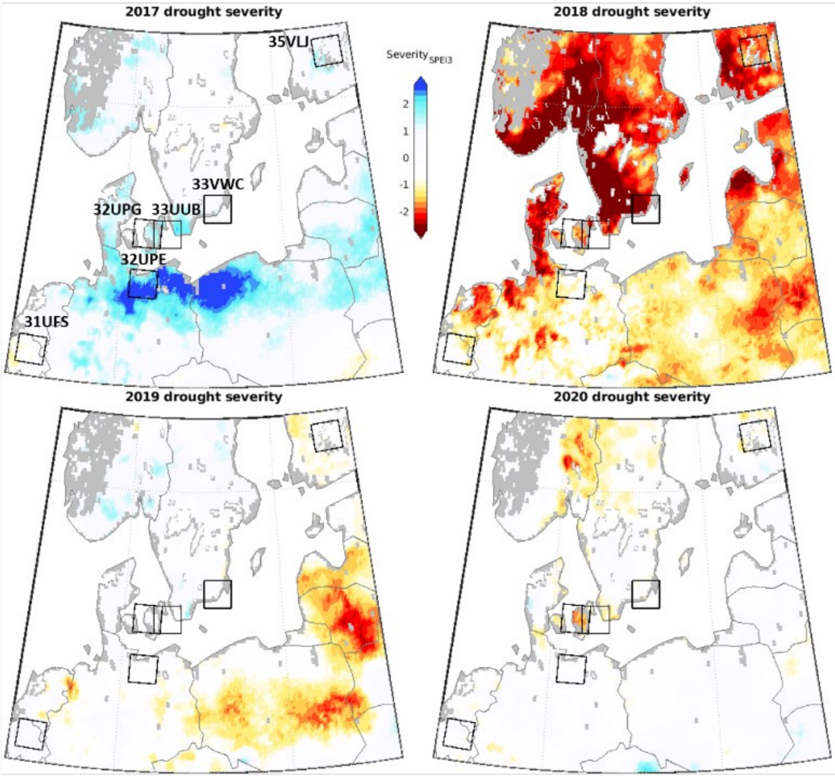

Figure 4 SPEI-3 drought severity for the study area. Reproduced from CLMS (2022) with permission.

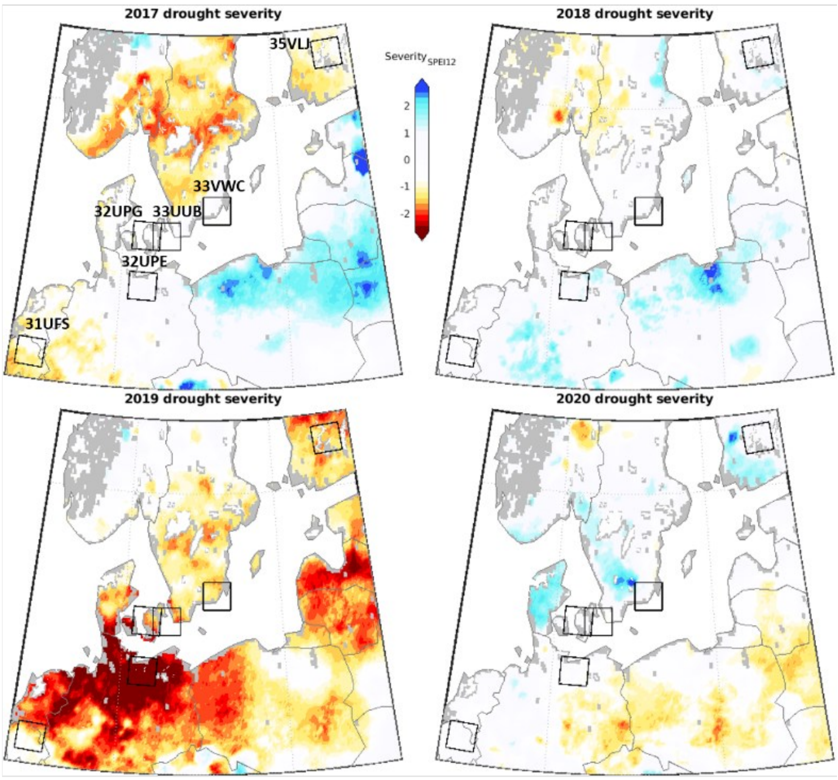

Figure 5. SPEI-12 drought severity for the study area. Reproduced from CLMS (2022) with permission.

3.2 Overall effect of SPEI on remotely sensed vegetation productivity

The relationship between SPEI and productivity, as estimated by annual values of total productivity, can be assessed by studying maps of total PPI productivity across the area, as shown in Figure 7. The map series indicates that the PPI pattern in 2018 resembles that of SPEI-3 in 2018, while the PPI pattern in 2019 is similar to that of SPEI12 in 2019. However, other factors such as variations in weather and land use practices may also influence the satellite-derived patterns. For example, the 2020 map suggests an effect in northern Germany and Benelux, not corresponding to any of the climate indices.

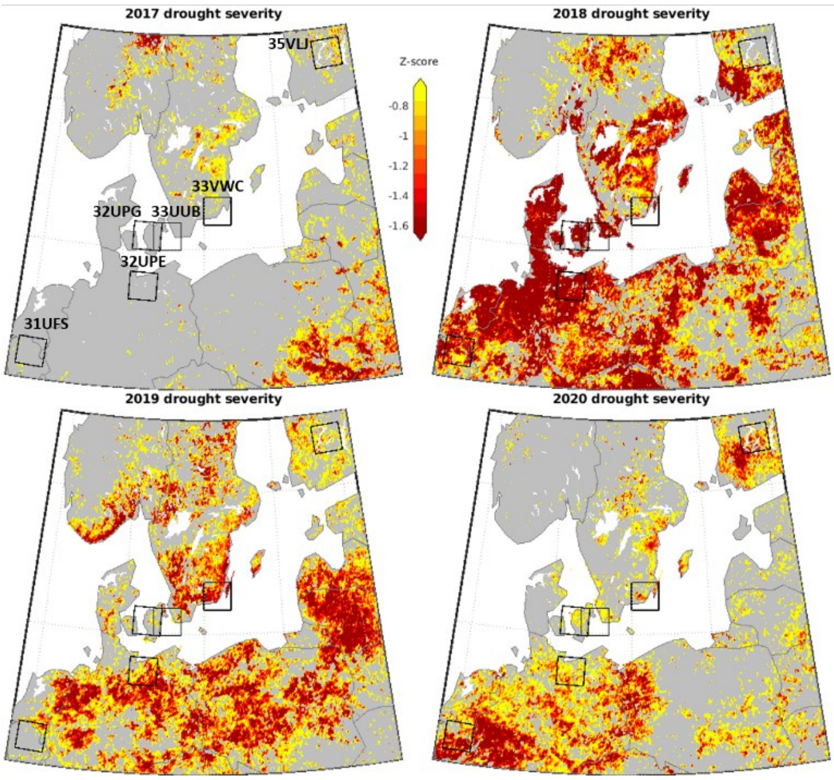

Figure 6. Z-scores of total PPI productivity estimated from detrended MODIS data mapped to 5 km resolution. Reproduced from CLMS (2022) with permission.

3.3 Drought impacts on croplands

The impact of severe drought on croplands in Southern Sweden can be seen in Figure 8. The SPEI-3 (black line) indicates a strong negative deviation starting from the beginning of 2018 and reaching its lowest point around August 1st. The PPI for different crops responds in two ways: lower peak values and a shift from uni-modal to bi-modal patterns. This bi-modal pattern is also observed in some crops in later years.

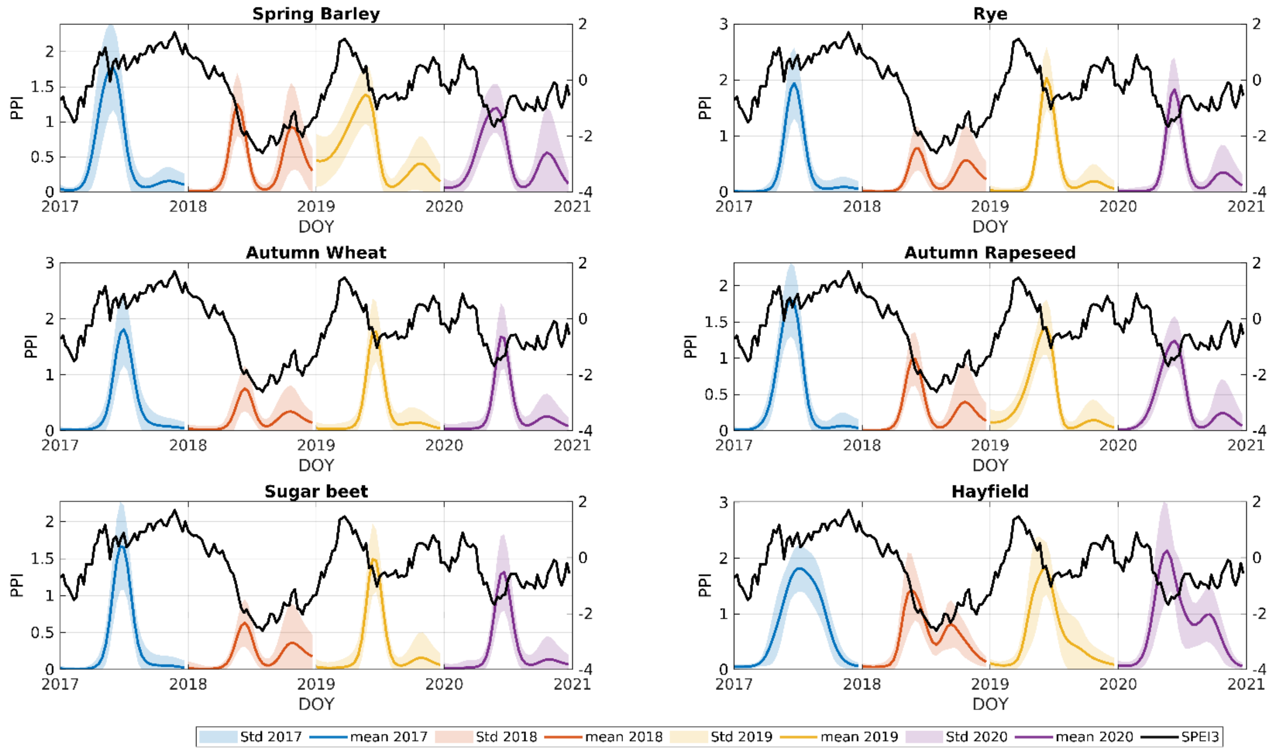

Figure 7. PPI seasonal trajectories (colored lines) and SPEI (black lines) for common crops in southern Sweden 2017-2020. Notice the discontinuous seasonal trajectories in different years due to the crop rotation. Reproduced from CLMS (2022) with permission.

The immediate drought effect on seasonal productivity in an intensively cropped area in S. Sweden is seen in Figure 9. It shows the general decline during 2018 in the productivity of the agricultural fields.

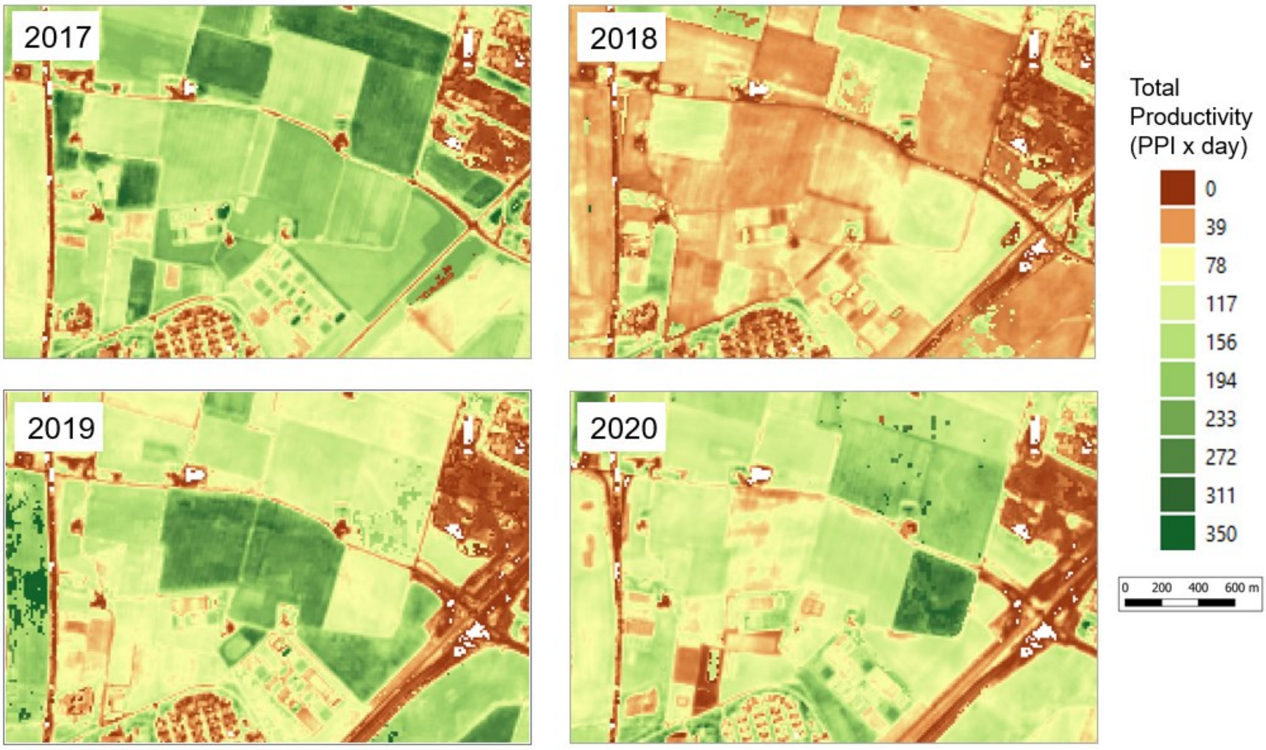

Figure 9. Seasonal integral (TPROD) of PPI for the years 2017-2020 for a small agricultural area in southern Sweden.

Figure 10 shows data that demonstrate the relationship between annual deviations in PPI total productivity for the area covered in Figure 2, versus official crop yield statistics for the administrative district covering the area (Skåne). In 2018, the lower yields (fluctuating around –30 % lower than the 4-year average for the different crops) correspond nearly perfectly with the lower PPI productivity (around –40% from the mean) in the same year. The relative relationships between different crops in 2018 match the two graphs.

3.4 Drought impacts on forest

The impact of drought on PPI is not as apparent for forest land as it is for agricultural land. Figure 11 displays annually aggregated PPI productivity data for the different study areas, separated for coniferous and deciduous forest pixels. It is evident that the productivity of conifers was neutral in 2018 compared to the mean, but showed some negative values, down to around -6%, in 2019. For deciduous forest pixels, productivity was slightly higher in 2018 but negative in 2019, around –10% from the mean.

Figure 10. Relative deviations of total productivity (TPROD) from the 2017-2020 mean values (top), and corresponding deviation in crop yield (kg/ha)(bottom). Reproduced from CLMS (2022) with permission.

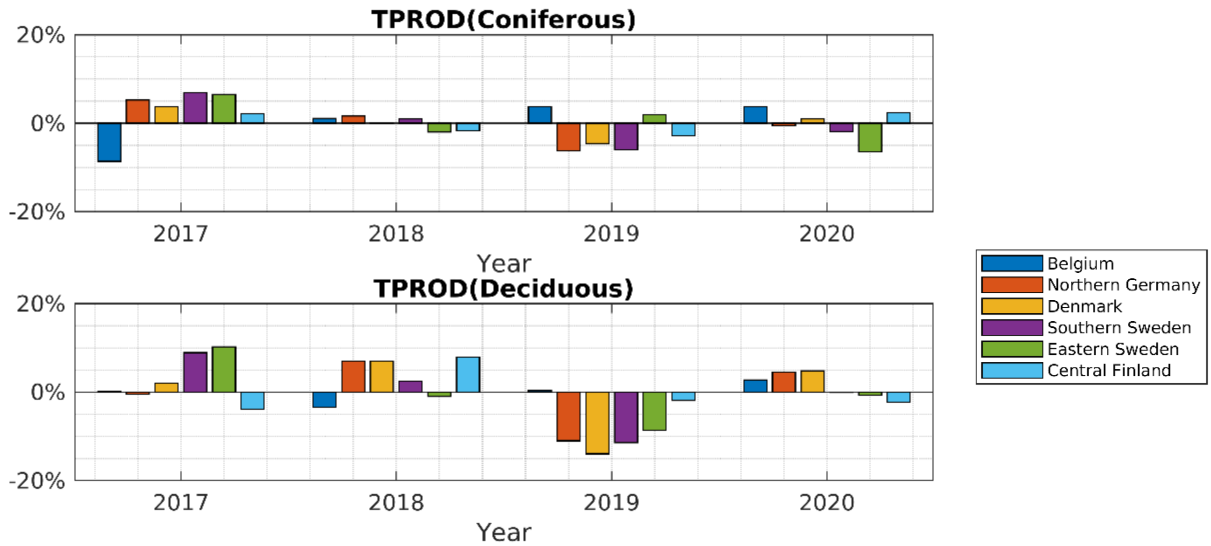

Figure 11. The relative deviation of total productivity (TPROD) for coniferous (top) and deciduous (bottom) forest lands across the different test areas. Reproduced from CLMS (2022) with permission.

To investigate the variation in total annual productivity across a small region in southern Sweden comprising forest, agricultural land, and an urban area, we created maps for each of the four years 2017-2020 (Figure 12). The forested area encompasses both broadleaf and coniferous stands. Our analysis reveals that during 2018, the productivity of the agricultural land (primarily grassland such as hayfields) experienced negative deviations, while forest productivity exhibited a slight increase. However, in 2019, we observed negative deviations in the forested area. Furthermore, the productivity in the agricultural land, predominantly grazing land, was highly negative in 2018.

Figure 13 depicts the variation in the length of the growing season. Notably, the forested areas experienced a considerably shorter growing season in the wet year of 2017, followed by a neutral or somewhat longer season in 2018 and 2019. There was no clear pattern in the agricultural areas regarding the duration of the growing season. We also found that the forested areas had an earlier start to the season in 2019 and a later end to the season in 2018. Furthermore, the end of the season in the hayfield was later during the drought year.

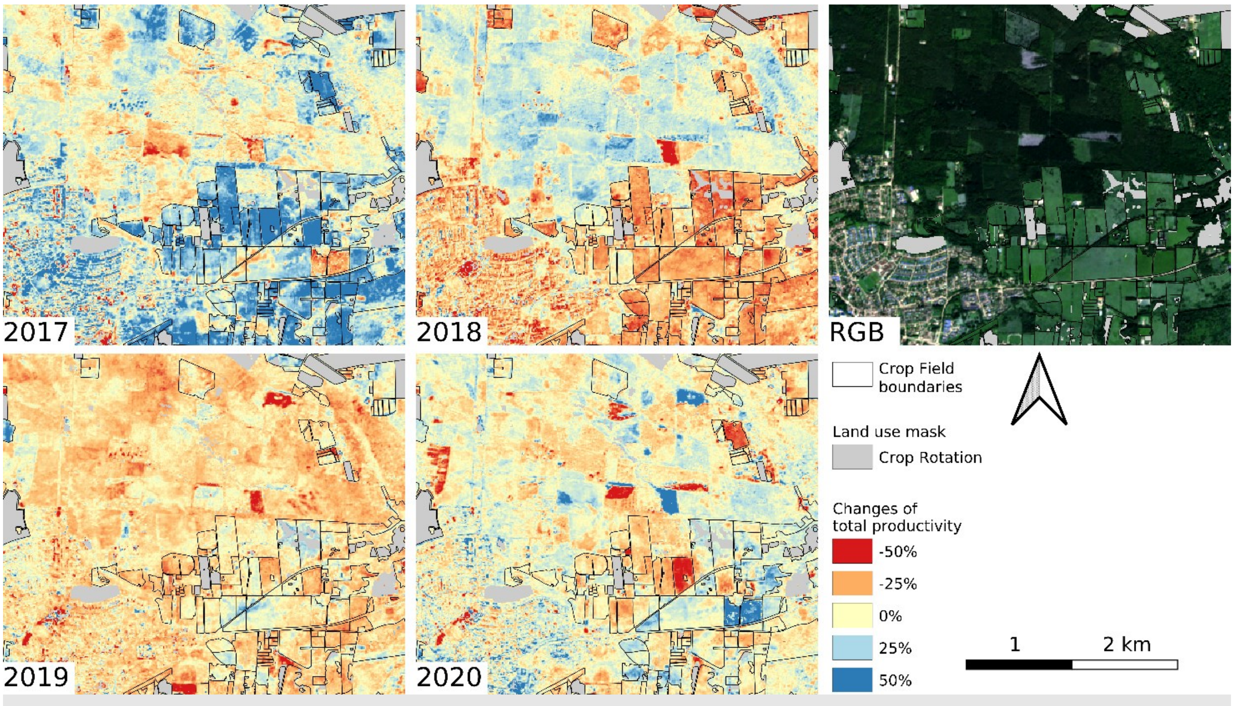

Figure 12. Annual deviations in total productivity (TPROD for both detected seasons) from the 2017-2020 mean values, along with an RGB image. Agricultural fields are delineated with black vectors, and areas under crop rotation are masked with grey patches. The area is located in southern Sweden centered at 55°41’10’’N, 13°21’40’’E. Reproduced from CLMS (2022) with permission.

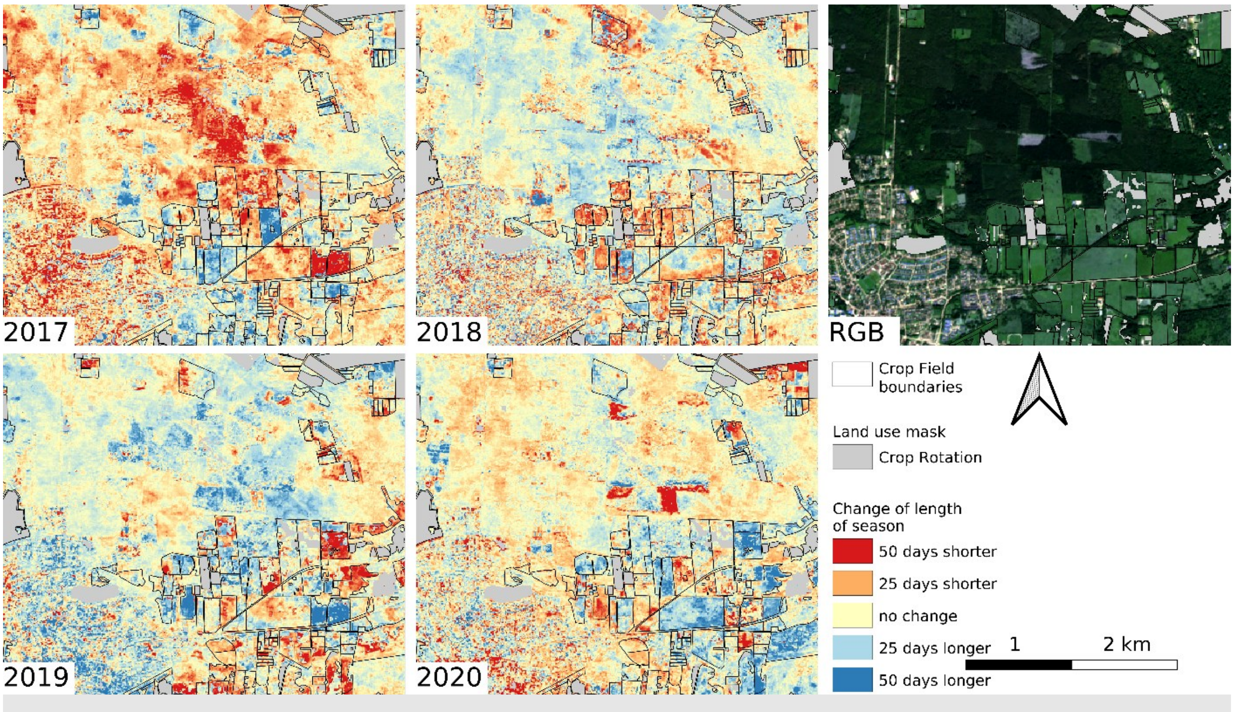

Figure 13. Annual deviations in season length (LENGTH) from the 2017-2020 mean values, along with an RGB image. Agricultural fields are delineated with black vectors, and areas under crop rotation are masked with grey patches. The area is located in southern Sweden centered at 55°41’10’’N, 13°21’40’’E. Reproduced from CLMS (2022) with permission.

4 Discussion

The study observed variations in phenology and productivity through the use of 10 m spatial resolution data used in the HR-VPP product, which are logical when compared with climate statistics expressed through the SPEI index and crop yield statistics. The 2018 drought had a direct and severe impact on crop yields, and the deviation in HR-VPP total productivity across crop fields in southern Sweden correlates well with official crop yield statistics, validating the total productivity (TPROD) parameter for assessing seasonal vegetation growth and biomass production.

In grasslands, the growing season during the drought was divided into two parts, possibly due to a return of rain in August, which provided moisture for a second greening of herbaceous vegetation before the winter. However, the pattern observed in some of the cropland may relate to the cropping cycle and cannot be explained without access to more detailed farming data.

In forest areas, total productivity responded only slightly during 2018, but there was a pronounced decline in 2019. This was consistent for five out of six analyzed areas. The negative deviation in 2019 was more prevalent on forest land than on open land, as shown by the deviation in medium-resolution PPI productivity data. (Figure 6). The delayed drought response in forests may be a result of a combination of several factors, including low soil water availability at the root level, damage to buds during the previous summer, change in carbon allocation, and modifications of the soil microbiota and structure. Such legacy effects have been shown to affect growth several years after drought (Huang et al. 2018; Kannenberg et al. 2020).

Drought effects on forest growth are rather complex and found to be more severe if the drought occurs during the dry season rather than the wet season (Huang et al. 2018), but it is also modulated by local conditions such as soil type, moisture, and elevation (Adams and Kolb 2005; Rehschuh et al. 2017). There is also some evidence that management activities, like thinning and mixing of species, may reduce drought sensitivity (Cabon et al. 2018; Laurent et al. 2003; Schäfer et al. 2019). The prolonged effect on water availability was shown by the SPEI-12 pattern that showed the strongest negative deviations in 2019 (Figure 5).

Drought impact due to increasing temperatures is an important factor limiting carbon uptake in N. American forests during the past century (Barber et al. 2000). With future increasing temperatures and possible increased risk of drought, the health and climate mitigating effect of northern forests may be seriously threatened.

The observation that forest PPI did not decrease during the drought year needs further analysis. However, it has been observed that leaf areas of beech (Fagus Sylvatica) increased rather than decreased during drought due to increased spring temperatures. Furthermore, the number of leaves in a tree is determined by the number of buds that are set in the previous summer period (Meier and Leuschner 2008), thus explaining the effect on PPI in the next rather than the present year. A recent analysis of the carbon cycle effects of the 2018 drought in northern Europe pointed to a mostly negative effect on forest gross primary productivity, but with varying size and signs across the 11 analyzed sites (Lindroth *et al.* 2020). The fact that much of this effect was related to surface conductance (Lindroth *et al.* 2020), would indicate that the drought affected the photosynthetic efficiency rather than the actual light absorption, explaining why PPI was not much affected. Thus, there is a likelihood that the productivity decrease in forests may be underestimated in the PPI data. The effect of low soil moisture on photosynthetic light use efficiency is a contributing factor to the systematic underestimation of drought impact on vegetation photosynthesis in remotely sensed products (Stocker *et al.* 2019).

5 Conclusions

The impacts of drought on crops and forests were analyzed in six areas across central and northern Europe. The effects of drought were clearly observable in Sentinel-2-derived products of high-resolution vegetation phenology and productivity (HR-VPP), including seasonal trajectories, phenology, and productivity parameters of HR-VPP. The total productivity (TPROD) was found to be the most sensitive parameter to the drought, particularly in croplands and forage grasslands (hayfield), where a significant decrease in TPROD correlated well with the decrease in crop yield per hectare reported by farmers in southern Sweden. This demonstrates the usefulness of seasonality parameters derived from Sentinel-2 data for monitoring agricultural disturbances due to drought.

In forested areas, the total productivity did not decrease during the drought year but was observed to decrease significantly the year after, particularly in deciduous forests. The decrease was correlated with SPEI-12, indicating a lag effect of one year. This observation is consistent with known mechanisms of drought impact on forest vegetation, such as disturbed bud formation, groundwater depletion, changes in soil microbiota and structure, etc., as reported in the literature. The study also observed changing phenology during and after the drought year, such as a prolonged growing season during the same year and an earlier growing season the next year. However, given the complex relationships between environment and tree growth, further studies are needed to fully understand these mechanisms and to assess the full utility of HR-VPP for drought impact assessment in forests.

The study highlights the importance of using remote sensing data to monitor and assess both regional and local scale impacts of drought on different land use types. It also underscores the need for more research to better understand the complex mechanisms that govern the responses of different ecosystems to drought, particularly forested ecosystems, and to improve the accuracy of drought impact assessments. Such information is crucial for developing effective strategies for mitigating the impacts of drought on agriculture and forest ecosystems in the face of future climate change.

6 References

Adams, H.D., & Kolb, T.E. (2005). Tree growth response to drought and temperature in a mountain landscape in northern Arizona, USA. *Journal of Biogeography, 32*, 1629-1640

Allen, R.G., Pereira, L.S., Raes, D., & Smith, M. (1998). Crop evapotranspiration - Guidelines for computing crop water requirements - FAO Irrigation and drainage paper 56. In. Rome: FAO

Anderegg, W.R.L., Hicke, J.A., Fisher, R.A., Allen, C.D., Aukema, J., Bentz, B., Hood, S., Lichstein, J.W., Macalady, A.K., McDowell, N., Pan, Y., Raffa, K., Sala, A., Shaw, J.D., Stephenson, N.L., Tague, C., & Zeppel, M. (2015). Tree mortality from drought, insects, and their interactions in a changing climate. *New Phytologist, 208*, 674-683

Barber, V.A., Juday, G.P., & Finney, B.P. (2000). Reduced growth of Alaskan white spruce in the twentieth century from temperature-induced drought stress. *Nature, 405*, 668-673

Beillouin, D., Schauberger, B., Bastos, A., Ciais, P., & Makowski, D. (2020). Impact of extreme weather conditions on European crop production in 2018. *Philosophical Transactions of the Royal Society B: Biological Sciences, 375*, 20190510

Boergens, E., Güntner, A., Dobslaw, H., & Dahle, C. (2020). Quantifying the Central European Droughts in 2018 and 2019 With GRACE Follow-On. *Geophysical Research Letters, 47*, e2020GL087285

Cabon, A., Mouillot, F., Lempereur, M., Ourcival, J.-M., Simioni, G., & Limousin, J.-M. (2018). Thinning increases tree growth by delaying drought-induced growth cessation in a Mediterranean evergreen oak coppice. *Forest Ecology and Management, 409*, 333-342

Cai, Z., Jönsson, P., Jin, H., & Eklundh, L. (2017). Performance of Smoothing Methods for Reconstructing NDVI Time-Series and Estimating Vegetation Phenology from MODIS Data. *Remote Sensing, 9*, 1271

Cammalleri, C., Naumann, G., Mentaschi, L., Formetta, G., Forzieri, G., Gosling, S., Bisselink, B., De Roo, A., & Feyen, L. (2020). Global warming and drought impacts in the EU. In, *JRC Technical report*. Luxembourg: Publications Office of the European Union

Carrão, H., Naumann, G., & Barbosa, P. (2016). Mapping global patterns of drought risk: An empirical framework based on sub-national estimates of hazard, exposure and vulnerability. *Global Environmental Change, 39*, 108-124

Christopoulou, A., Sazeides, C.I., & Fyllas, N.M. (2021). Size-mediated effects of climate on tree growth and mortality in Mediterranean Brutia pine forests. *Science of the Total Environment*, 151463

Ciais, P., Reichstein, M., Viovy, N., Granier, A., Ogée, J., Allard, V., Aubinet, M., Buchmann, N., Bernhofer, C., Carrara, A., Chevallier, F., De Noblet, N., Friend, A.D., Friedlingstein, P., Grünwald, T., Heinesch, B., Keronen, P., Knohl, A., Krinner, G., Loustau, D., Manca, G., Matteucci, G., Miglietta, F., Ourcival, J.M., Papale, D., Pilegaard, K., Rambal, S., Seufert, G., Soussana, J.F., Sanz, M.J., Schulze, E.D., Vesala, T., & Valentini, R. (2005). Europe-wide reduction in primary productivity caused by the heat and drought in 2003. *Nature, 437*, 529

CLMS (2022). High Resolution Vegetation Phenology and Productivity, Use Case: Local Scale Impacts of the 2018 Drought on Vegetation in N. Europe. In: European Environment Agency (EEA)

Conradt, T., Engelhardt, H., Menz, C., Vicente-Serrano, S.M., Farizo, B.A., Peña-Angulo, D., Domínguez-Castro, F., Eklundh, L., Jin, H., Boincean, B., Murphy, C., & López-Moreno, J.I. (2023). Cross-sectoral impacts of the 2018–2019 Central European drought and climate resilience in the German part of the Elbe River basin. *Regional Environmental Change, 23*, 32

Dracup, J.A., Lee, K.S., & Paulson Jr., E.G. (1980). On the definition of droughts. *Water Resources Research, 16*, 297-302

Huang, M., Wang, X., Keenan, T.F., & Piao, S. (2018). Drought timing influences the legacy of tree growth recovery. *Global Change Biology, 24*, 3546-3559

Huang, W., & Wang, H. (2021). Drought and intensified agriculture enhanced vegetation growth in the central Pearl River Basin of China. *Agricultural Water Management, 256*, 107077

Humphrey, V., Zscheischler, J., Ciais, P., Gudmundsson, L., Sitch, S., & Seneviratne, S.I. (2018). Sensitivity of atmospheric CO_2 growth rate to observed changes in terrestrial water storage. *Nature, 560*, 628-631
Jin, H., & Eklundh, L. (2014). A physically based vegetation index for improved monitoring of plant phenology. *Remote Sensing of Environment, 152*, 512-525
Kannenberg, S.A., Schwalm, C.R., & Anderegg, W.R.L. (2020). Ghosts of the past: how drought legacy effects shape forest functioning and carbon cycling. *Ecology Letters, 23*, 891-901
Lafleur, P.M., & Humphreys, E.R. (2018). Tundra shrub effects on growing season energy and carbon dioxide exchange. *Environmental Research Letters, 13*, 055001
Laurent, M., Antoine, N., & Joël, G. (2003). Effects of different thinning intensities on drought response in Norway spruce (Picea abies (L.) Karst.). *Forest Ecology and Management, 183*, 47-60
Lawal, S., Hewitson, B., Egbebiyi, T.S., & Adesuyi, A. (2021). On the suitability of using vegetation indices to monitor the response of Africa's terrestrial ecoregions to drought. *Science of The Total Environment, 792*, 148282
Lindroth, A., Holst, J., Linderson, M.-L., Aurela, M., Biermann, T., Heliasz, M., Chi, J., Ibrom, A., Kolari, P., Klemedtsson, L., Krasnova, A., Laurila, T., Lehner, I., Lohila, A., Mammarella, I., Mölder, M., Löfvenius, M.O., Peichl, M., Pilegaard, K., Soosaar, K., Vesala, T., Vestin, P., Weslien, P., & Nilsson, M. (2020). Effects of drought and meteorological forcing on carbon and water fluxes in Nordic forests during the dry summer of 2018. *Philosophical Transactions of the Royal Society B: Biological Sciences, 375*, 20190516
Maxmen, A. (2013). Crop pests: Under attack. *Nature, 501*, S15-S17
Meier, I.C., & Leuschner, C. (2008). Leaf Size and Leaf Area Index in Fagus sylvatica Forests: Competing Effects of Precipitation, Temperature, and Nitrogen Availability. *Ecosystems, 11*, 655-669
Mishra, A.K., & Singh, V.P. (2010). A review of drought concepts. *Journal of Hydrology, 391*, 202-216
Mokhtar, A., He, H., Alsafadi, K., Mohammed, S., Ayantobo, O.O., Elbeltagi, A., Abdelwahab, O.M.M., Zhao, H., Quan, Y., Abdo, H.G., Gyasi-Agyei, Y., & Li, Y. Assessment of the effects of spatiotemporal characteristics of drought on crop yields in southwest China. *International Journal of Climatology, n/a*
Naumann, G., Cammalleri, C., Mentaschi, L., & Feyen, L. (2021). Increased economic drought impacts in Europe with anthropogenic warming. *Nature Climate Change, 11*, 485-491
Oldfield, E.E., Eagle, A.J., Rubin, R.L., Rudek, J., Sanderman, J., & Gordon, D.R. (2022). Crediting agricultural soil carbon sequestration. *Science, 375*, 1222-1225
Peters, W., Bastos, A., Ciais, P., & Vermeulen, A. (2020). A historical, geographical and ecological perspective on the 2018 European summer drought. *Philosophical Transactions of the Royal Society B: Biological Sciences, 375*, 20190505
Rehschuh, R., Mette, T., Menzel, A., & Buras, A. (2017). Soil properties affect the drought susceptibility of Norway spruce. *Dendrochronologia, 45*, 81-89
Rinne, J., Tuovinen, J.-P., Klemedtsson, L., Aurela, M., Holst, J., Lohila, A., Weslien, P., Vestin, P., Łakomiec, P., Peichl, M., Tuittila, E.-S., Heiskanen, L., Laurila, T., Li, X., Alekseychik, P., Mammarella, I., Ström, L., Crill, P., & Nilsson, M.B. (2020). Effect of the 2018 European drought on methane and carbon dioxide exchange of northern mire ecosystems. *Philosophical Transactions of the Royal Society B: Biological Sciences, 375*, 20190517
Santini, M., Noce, S., Antonelli, M., & Caporaso, L. (2022). Complex drought patterns robustly explain global yield loss for major crops. *Scientific Reports, 12*, 5792
SCB (2018). Production of cereal crops, dried pulses and oilseed crops in 2018. Preliminary results for the whole country. In, *Sveriges officiella statistik Statistiska meddelanden* (p. 20): Statistiska Centralbyrån
Schäfer, C., Rötzer, T., Thurm, E.A., Biber, P., Kallenbach, C., & Pretzsch, H. (2019). Growth and Tree Water Deficit of Mixed Norway Spruce and European Beech at Different Heights in a Tree and under Heavy Drought. *Forests, 10*, 577
Stocker, B.D., Zscheischler, J., Keenan, T.F., Prentice, I.C., Seneviratne, S.I., & Peñuelas, J. (2019). Drought impacts on terrestrial primary production underestimated by satellite monitoring. *Nature Geoscience, 12*, 264-270

Vicente-Serrano, S.M., Beguería, S., & López-Moreno, J.I. (2010). A multiscalar drought index sensitive to global warming: the standardized precipitation evapotranspiration index. *Journal of Climate, 23*, 1696-1718

Zhong, S., Sun, Z., & Di, L. (2021). Characteristics of vegetation response to drought in the CONUS based on long-term remote sensing and meteorological data. *Ecological Indicators, 127*, 107767